Accepted Manuscript

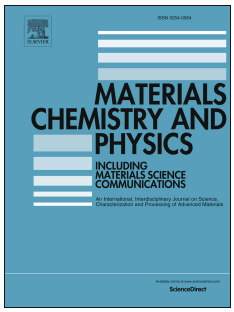

Synthesis and ceramic conversion of novel silazane modified phenol formaldehyde resin

T. Ganesh Babu, S. Bhuvaneswari, Renjith Devasia

PII: S0254-0584(18)30194-9

DOI: 10.1016/j.matchemphys.2018.03.031

Reference: MAC 20434

To appear in: *Materials Chemistry and Physics*

Received Date: 15 October 2017

Revised Date: 8 March 2018

Accepted Date: 11 March 2018

Please cite this article as: T. Ganesh Babu, S. Bhuvaneswari, R. Devasia, Synthesis and ceramic conversion of novel silazane modified phenol formaldehyde resin, *Materials Chemistry and Physics* (2018), doi: 10.1016/j.matchemphys.2018.03.031.

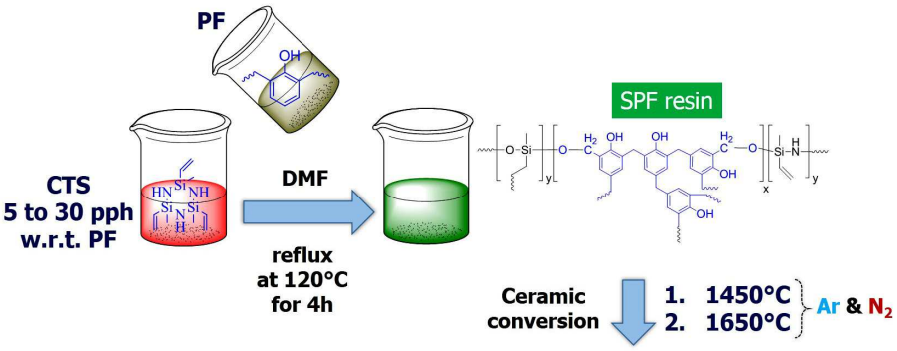

Under Ar atm. at 1450°C & 1650°C

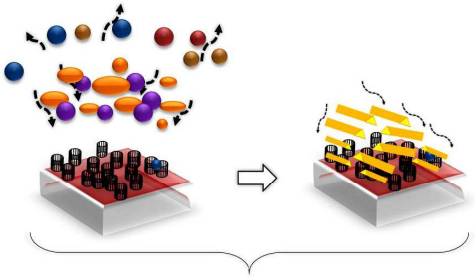

Macro porous SiOC ceramics & 1D Nano-rods SiC ceramics were obtained

Under N_2 atm. at 1450°C & 1650°C

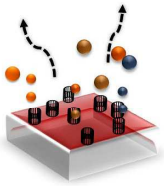

Macro porous Si_3N_4/SiC ceramics were obtained

Synthesis and ceramic conversion of novel silazane modified phenol formaldehyde resin

Ganesh Babu T.[a], Bhuvaneswari S.[b] and Renjith Devasia[a,*]

[a]Ceramic Matrix Products Division, Analytical, Spectroscopy and Ceramics Group, PCM Entity, Vikram Sarabhai Space Centre, ISRO, Kerala, India-690522

[b]Analytical and Spectroscopy Division, Analytical, Spectroscopy and Ceramics Group, PCM Entity, Vikram Sarabhai Space Centre, ISRO, Kerala, India-690522

[*]Corresponding author: Tel: +91471 2563870, Fax: +91471 2564096

E-mail address: renjithdevasia@gmail.com

ABSTRACT

Novel silazane modified phenol formaldehyde (SPF) resins were synthesized by reacting varying amounts of 1, 3, 5-trimethyl-1', 3', 5'-trivinylcyclotrisilazane (CTS) with phenol formaldehyde (PF) resin. For the selection of an appropriate pyrolysis condition, polymer-to-ceramic conversion of SPF was carried out at 1450°C and 1650°C under argon and nitrogen atmosphere. The pyrolysis conditions significantly affected the evolution of ceramic phases, excess carbon and morphology which were thoroughly investigated through XRD, Raman and FESEM techniques. This study establishes silazane modified phenol formaldehyde as a new class of preceramic polymer for high-temperature applications. The study also reveals that nitrogen atmosphere is a more suitable gas atmosphere than argon atmosphere for preparation of desired C/Si_3N_4/SiC ceramics with higher ceramic yield.

Keywords: *Silazane modified phenol formaldehyde resin; SiCN ceramic; pyrolysis condition; C/*Si_3N_4/SiC *ceramic composites; high-temperature*

Graphical abstract

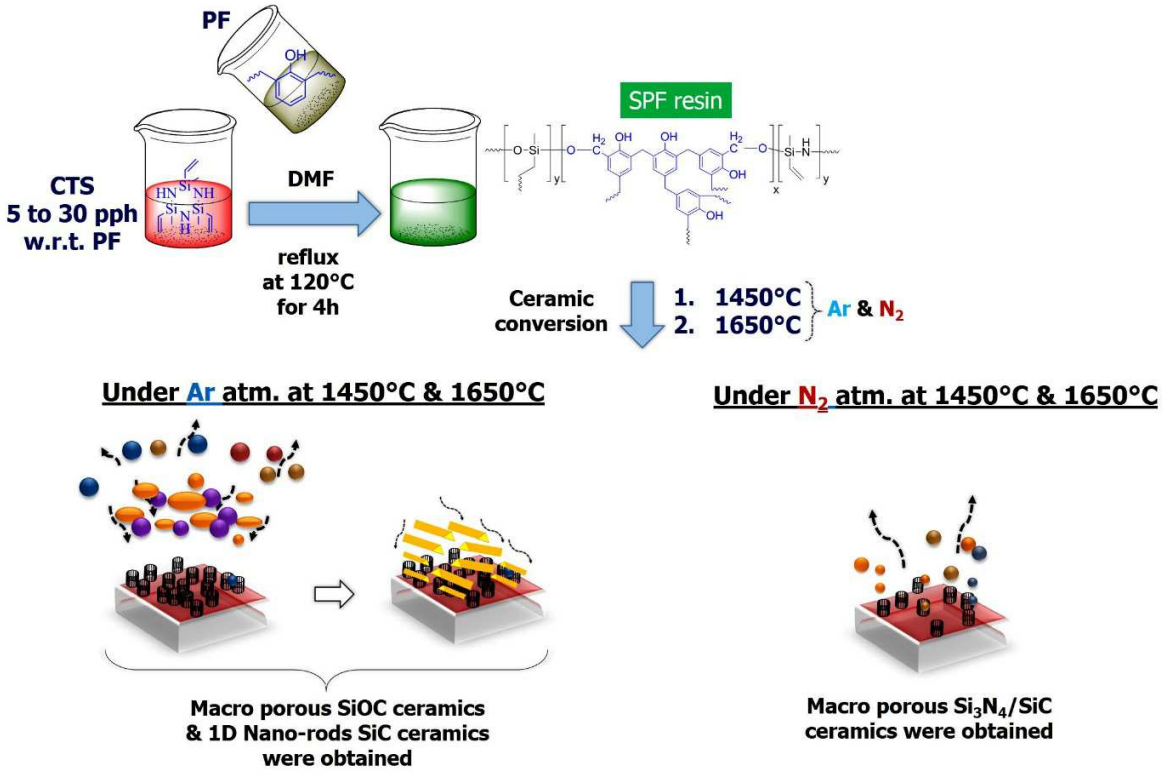

1. Introduction

With the rapid advancement in high temperature applications such as rocket nozzles, aeronautic jet engines, heat shields and aircraft braking systems, more and more materials are extensively explored that can survive at the extreme environments [1-3]. Recently, polymer derived ceramics (PDC) based on silicon carbonitrides (SiCN) have attracted enormous attention due to their superior properties, such as high-temperature stability, oxidation and corrosion resistance, as well as enhanced thermo-mechanical, electrical, magnetic, and optical properties [4-8]. Among the several strategies to produce Si-C-N based preceramic polymers from monomers [7, 9], one of particular interest is the polymerization of vinyl substituents from molecular vinylsilazanes by free radical polymerization. This mechanism was first studied by Toreki*et al* [10] by using 1, 3, 5-trimethyl-1',3',5'-trivinylcyclotrisilazane (CTS) as the starting material. This silazane is commercially available and is relatively inexpensive. However, the resultant polycyclotrisilazane (PCTS) was insoluble in common solvents, which limits further processability and impedes its use as a preceramic resin for high-temperature applications. This difficulty in further processing of preceramic resins can be overcome by its modification with organic resins.

Among various organic resins, phenol-formaldehyde (PF) resin can easily be modified with inorganic moieties such as boron [11], silicon [12], titanium [13] and phosphorus [14]. These modified resins were widely used in the process of polymer infiltration and pyrolysis technique to prepare refractory carbide modified carbon/carbon composites (C/C) [15-18]. However, similar to the disadvantages associated with other polymeric materials, the application of PF resin at high temperatures is restricted due to its thermal degradation above 200°C [19].

For the development of advanced ceramics based on modification of preceramic resin with organic resin such as PF, it is particularly attractive to utilize the best properties of each component to develop new materials with tailor made properties. In this regard, phenol formaldehyde resin modified with silazane is expected to result in advanced preceramic resin having higher solubility and thermal stability.

Many reports are available on PF resin based preceramic matrix resin, of which organometallic polymers, such as polysiloxanes [20, 21] and polyborosiloxane [22], were widely studied for improving the thermo-structural properties of high-performance materials. To the best of our knowledge, there are no available reports on silazane modified phenol formaldehyde (SPF) based preceramic resin. Also, the conversion of preceramic resin to ceramics with high yield (>60 wt. %) and tailor-ability to obtain the desired ceramics are important criteria for high-temperature applications. These criteria are highly dependent on the molecular structure and the pyrolysis conditions (temperature and atmosphere) of the preceramic resin, which significantly alters their properties for high-temperature applications [23, 24]. Furthermore, SiCN based ceramics are largely employed in the field of ceramic matrix and composites (CMCs) and coating applications. In this regard, the most commonly employed pyrolysis gas atmospheres are argon and nitrogen. Though, ammonia is another suggested pyrolysis atmosphere, the degradation of the reinforcement like carbon fibre is quite feasible under corrosive ammonia atmosphere [25] which results in the deterioration of the CMCs strength making ammonia gas atmosphere highly unsuitable for CMCs and coating high-temperature applications. Hence, this study was carried out under argon and nitrogen atmosphere for the final intended application and to select the most suitable pyrolysis condition to achieve desired ceramics in high yield.

Here, we report synthesis and ceramic conversion of a novel preceramic polymer system based on silazane modified phenol formaldehyde resin (SPF). This preceramic polymer was synthesized by reacting varying amounts of 1, 3, 5-trimethyl-1', 3', 5'-trivinylcyclotrisilazane (CTS) with phenol formaldehyde (PF) resin and the effect of pyrolysis conditions on ceramic yield, structural evolution and preceramic crystallization behavior was thoroughly investigated. The ultimate objective of this study was to assess the potential of SPF as a preceramic resin for high-temperature applications and selection of an appropriate pyrolysis condition in order to achieve desired ceramic in high yield (>60 wt. %).

2. Experimental

2.1 Materials

Silazane modified phenol formaldehyde (SPF) resins were synthesized by the reaction of PF resin (produced in-house; see supporting information (S), S-Table 1) with 1, 3, 5-trimethyl-1', 3', 5'-trivinylcyclotrisilazane (CTS) (99.5 % purity, Sigma Aldrich, Bangalore, India), dicumyl peroxide (DCP) as catalyst (98% purity, SD fine-Chem Ltd., Mumbai, India), toluene (99.9% purity, Sigma Aldrich, Bangalore, India) and N, N-dimethylformamide (DMF) (99.9% purity, Sigma Aldrich, Bangalore, India) as solvents.

2.2 Synthesis of silazane modified phenol formaldehyde (SPF) resin

SPF resins with different concentration of silazane were synthesized *via* a facile two step reaction (Scheme 1). As a typical example, in the first step, preparation of polycyclotrisilazane (PCTS) was carried out according to a previously reported procedure [10]. Five gram of CTS was reacted with 0.06 g of DCP (CTS: DCP= 90: 1 molar ratio) in dry toluene. The reaction mixture was refluxed at 135°C for 12h under nitrogen atmosphere to form viscous PCTS resin. In the second step, 100 g of PF resin in DMF was added drop-wise to the obtained PCTS resin

and refluxed at 120°C for 4h under nitrogen atmosphere. Finally, yellowish viscous SPF resins was obtained which is designated as SPF-5 [CTS is 5 parts per hundred (pph) w.r.t. PF]. Similarly, SPF-10, SPF-15, SPF-20, SPF-25 and SPF-30 resins were also prepared by varying the concentration of CTS from 10 pph to 30 pph w.r.t. PF, respectively (as shown in S-Table 2). However, the concentration of CTS could not be increased beyond 30 pph due to incomplete reaction of PCTS with PF resulting in the formation of separate phase in the reaction medium.

2.3 Methods

The structural characterization of SPF resin was done using FT-IR (Perkin Elmer Spectrum GX spectrometer) and NMR (Bruker DMX 300 Spectrometer) analysis. The ^{1}H NMR spectra were measured at 300 MHz, with chemical shifts determined in $CDCl_3$ relative to 7.26 ppm and ^{29}Si NMR spectra were measured at 60MHz. The structural evolution of the resultant ceramics were studied using X-ray diffraction (XRD, Bruker D8 discover) with Cu-Kα radiation (40kV, 40mA; step scan of 0.051, counting time of 5s/step and 1.5460 Å). The structural organization of excess carbon in the ceramics were investigated using Raman spectra recorded with WITec alpha 300R confocal Raman microscope using frequency doubled Nd: YAG laser of excitation wavelength 532 nm. The morphological features were studied using Field Emission Scanning Electron Microscopy (FESEM, Carl Zeiss, Supra 55, Germany). The digitally stored images thus obtained from FESEM were further processed using “ImageJ” image processing and analysis software for the surface porosity measurement [26, 27]. The elemental composition of ceramics were determined by wet chemical analysis method [28].

2.4 Pyrolysis condition

For the selection of an appropriate pyrolysis condition, polymer-to-ceramic conversion of SPF was carried out at 1450°C and 1650°C separately under argon and nitrogen atmosphere. Ceramic conversion studies were carried out by heating the sample at a rate of 3°C/min and

maintained at pyrolysis temperature (1450°C or 1650°C) for 3 h. The furnace was then cooled back to room temperature at a rate of 3°C/min. Both the heating and cooling process were carried out under argon or nitrogen atmosphere at a flow rate of 50 mL/min.

3. Results and Discussion

3.1 Synthesis and characterization of SPF resin

The first step involved the formation of PCTS by the reaction of CTS with DCP (Step-1 in Scheme 1). Figure 1(a) shows the FT-IR spectra of CTS and PCTS.

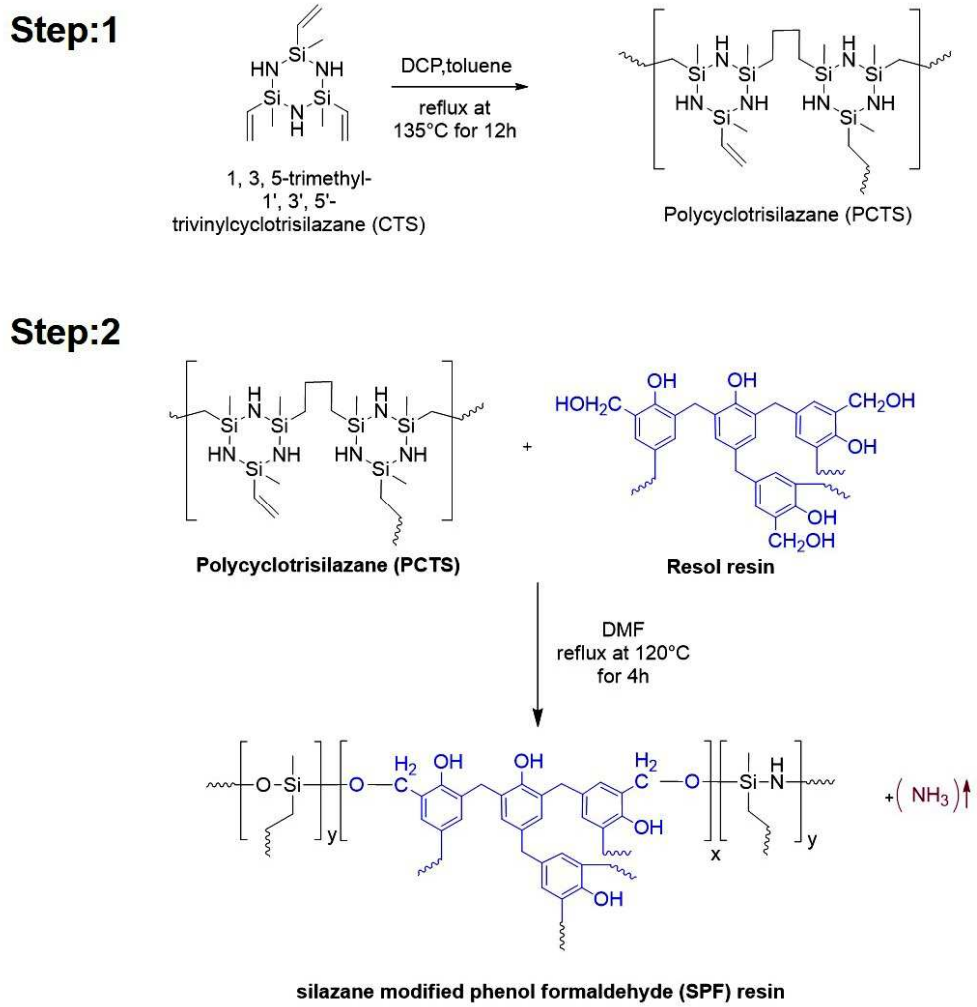

Scheme 1. Synthesis of SPF resin

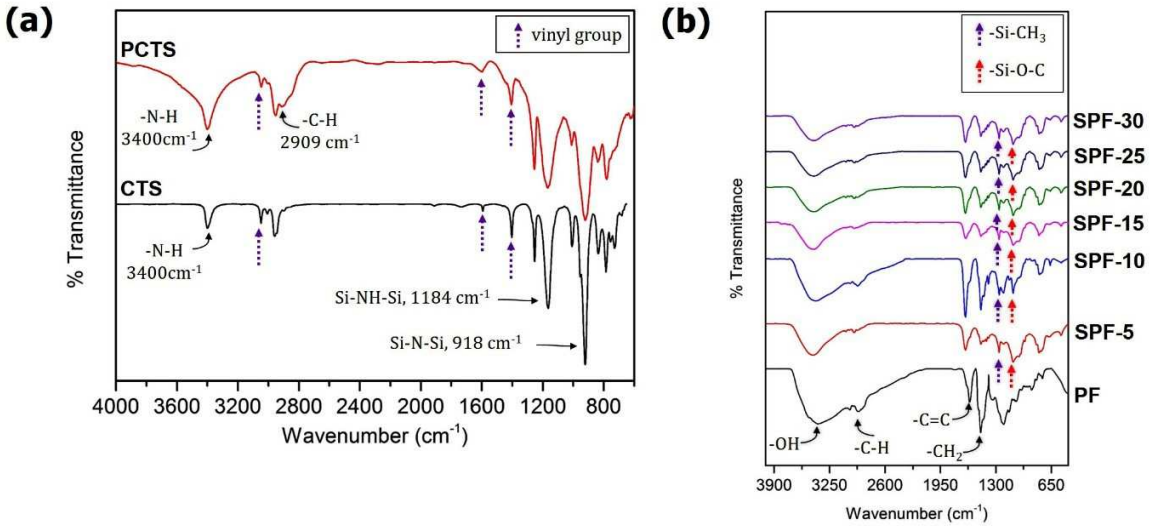

Figure 1. FT-IR spectra of (a) CTS and PCTS resin and (b) PF resin and different composition of SPF resins

As expected, both showed similar spectrum, however, in the PCTS spectrum a new band corresponding to aliphatic C-H stretching appeared at 2909 cm^{-1}. Also, with the appearance of an aliphatic C-H stretching band, decrease in the band intensities of the vinyl groups at 3047 cm^{-1}, 1594 cm^{-1} and 1401 cm^{-1} was observed which indicates that vinyl polymerization has occurred partially. Additionally, broadening of the N–H stretching band (3400 cm^{-1}) as well as the Si–N–Si stretching (918 cm^{-1}) were observed which further confirms polymerization of CTS to form PCTS resin.

In the second step, formation of SPF resins occurs by the reaction of PCTS with PF (Step-2 in Scheme 1). Figure 1(b) shows FT-IR spectra of PF and silazane modified PF resins. The appearance of Si-O-C and Si-C-H bands at 1268 cm^{-1} and 1093 cm^{-1}, respectively, confirms the reaction proceeds through condensation reaction of PCTS with PF. Moreover, by increasing the concentration of PCTS, the intensity of Si–O–C stretching band increases which proves beyond doubt that PCTS has chemically reacted with PF resin to form SPF resin.

Further, the detailed reaction mechanism for the formation of SPF resins was discerned through NMR analysis. The ^{1}H NMR spectra of SPF resin shows signals corresponding to $SiCH_3$ group at δ = 0-0.45 ppm, -CH_2- group at δ = 3.43-3.92 ppm, methyloyl -CH_2- group at δ =4.80-4.76 ppm, -CH_2=CH- at δ = 5.71–6.28 ppm, Ar-H at δ = 6.74-6.85 ppm, and phenolic -OH group at δ = 7.37 ppm (Figure 2). However, peaks corresponding to methyloyl -OH group at δ = 7.03 ppm and N-H group at δ = 0.62 ppm, typical signals for PF and PCTS resins (Figure S1), respectively were not observed in the spectra. This confirms the reaction of PCTS with methylol -OH groups of PF which precedes over phenolic -OH groups of PF, with evolution of ammonia as shown in Scheme 1.

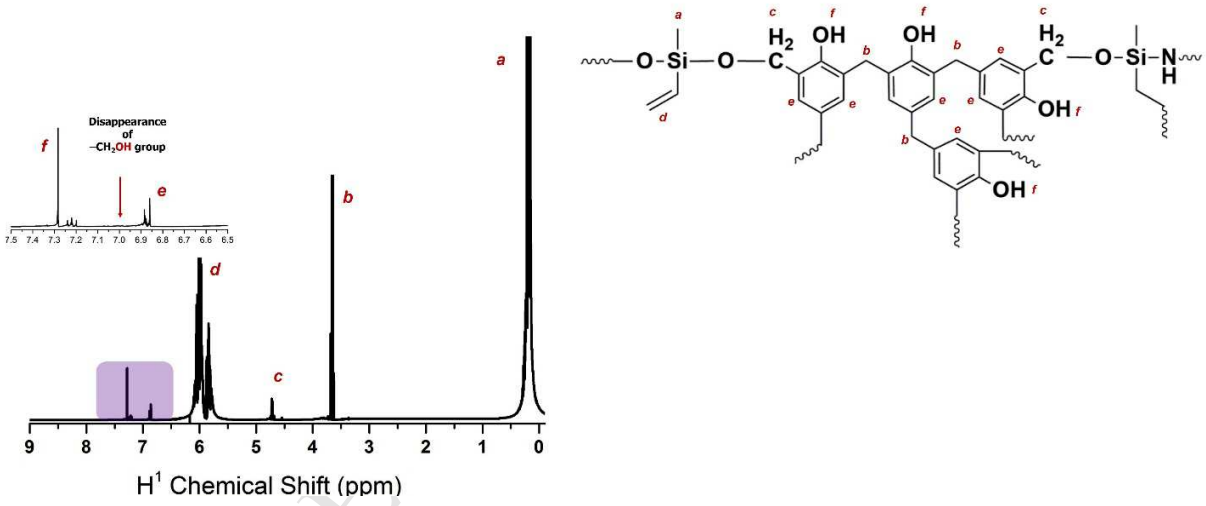

Figure 2. ^{1}H NMR spectra of SPF resin

The validation of reaction mechanism was further done through ^{29}Si NMR studies. Figure S2 (a) and (b) shows ^{29}Si NMR spectra of PCTS and SPF. PCTS showed SiC_2N_2 signal at δ = -14.90 ppm, whereas in SPF no signal for SiC_2N_2 was observed. However, two new peaks at δ = -32.55 ppm and δ = -35.02 ppm were observed for SPF, which corresponds to SiC_2NO and

SiC_2O_2, respectively. The formation of SiC_2NO and SiC_2O_2 indicates that, the reaction of PCTS with PF proceeds through a ring opening mechanism as shown in Scheme 2.

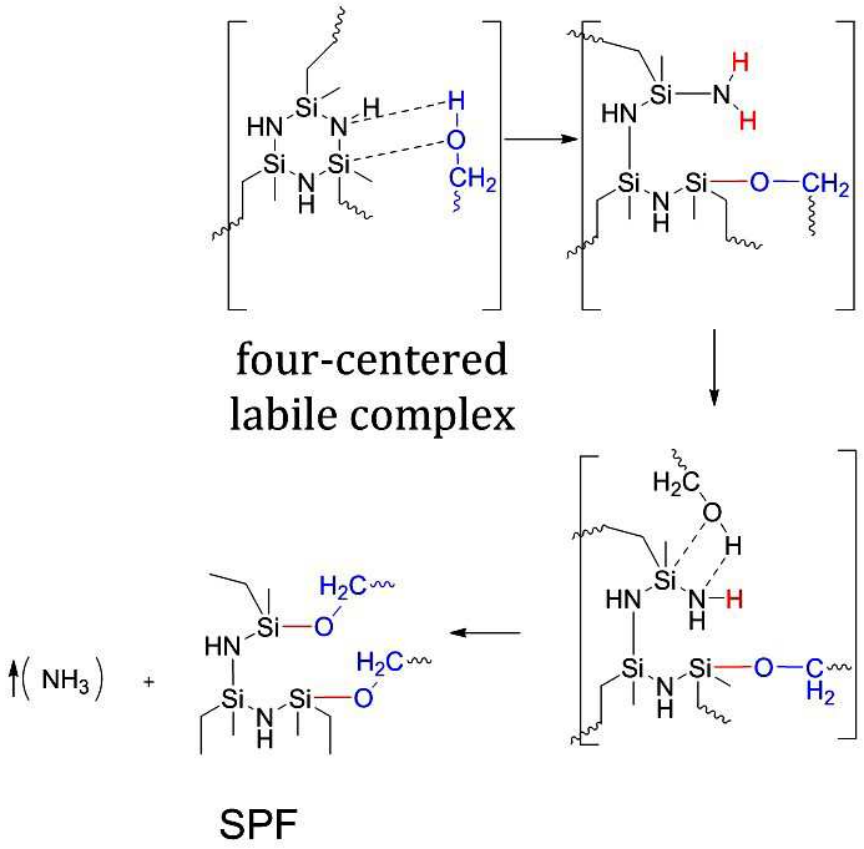

Scheme 2. Proposed ring opening mechanism for the formation of SPF resin

The ring opening proceeds *via* condensation of one Si-NH-Si linkage of PCTS with two methyloyl -OH groups of PF which occurs in two steps. In the first step, the electrophilic attack of the hydrogen atoms of the methyloyl -OH group of PF on the nitrogen atoms of the silazane occurs to form a four centered labile complex. Formation of one Si-O-C linkage and one $Si\text{-}NH_2$ group occurs by the splitting of Si-N bond in the complex. In the second step, the formed $Si\text{-}NH_2$ group undergoes further reaction with methyloyl -OH group of PF forming another Si-O-C

linkage with the evolution of NH_3 gas. This results in a more stable and less strained linear structured SPF resin.

3.2 Pyrolysis of SPF resin

To evaluate the potential of SPF resin as a preceramic polymer for high-temperature applications, studies on pyrolysis condition are mandatory. To meet this objective, Polymer-to-ceramic conversion was carried out under different pyrolysis conditions (*see Section- 2.4*). The thermal stability of the resultant ceramics in terms of thermal decomposition, crystallization, and ceramic yield under different pyrolysis condition were investigated through XRD, Raman and FESEM techniques.

3.2.1 XRD of pyrolyzed SPF resin

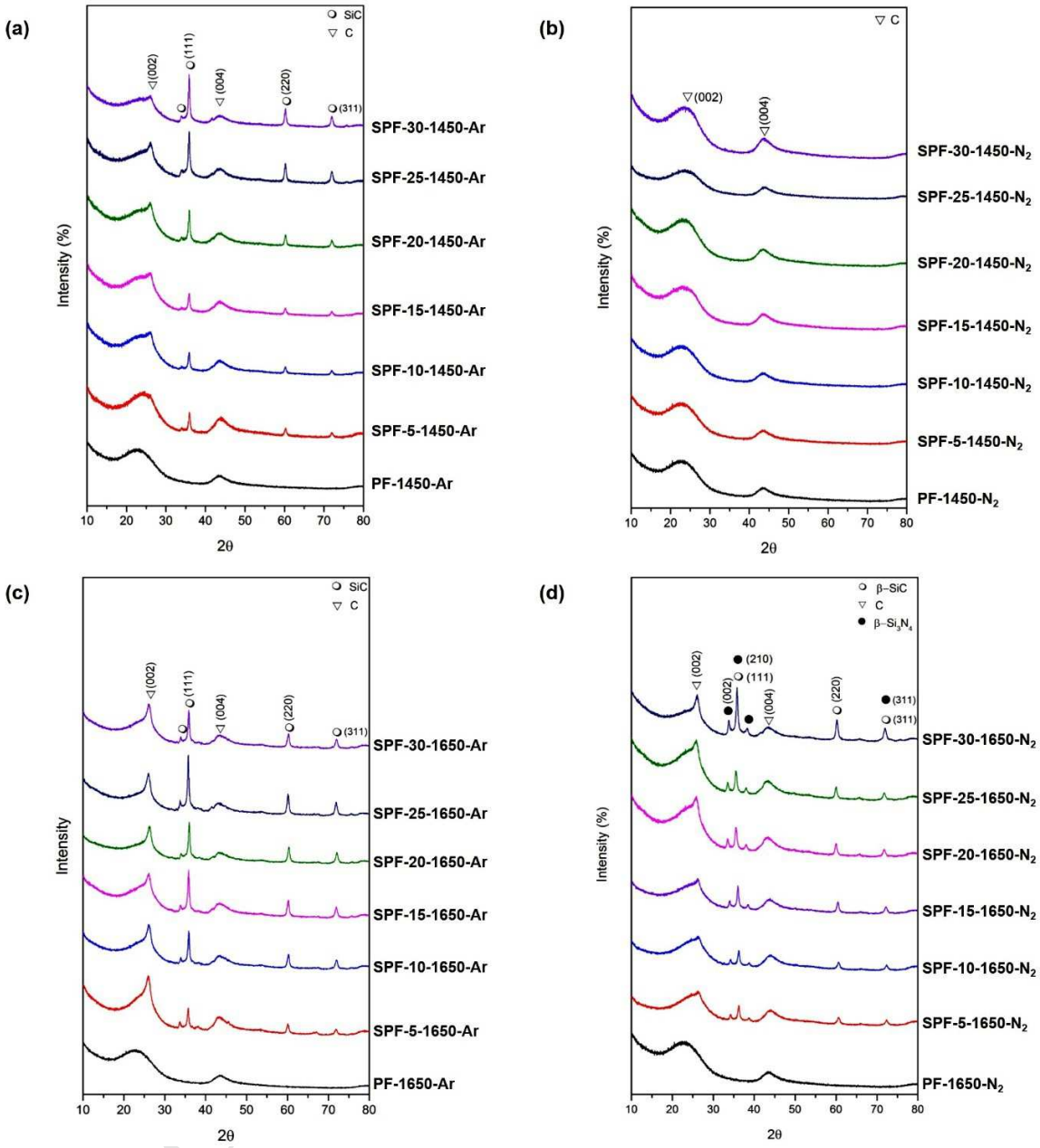

Figure 3. XRD spectra of the pyrolyzed SPF resin (a) argon atmosphere at 1450°C (b) nitrogen atmosphere at 1450°C and (c) argon atmosphere at 1650°C (d) nitrogen atmosphere at 1650°C

Figure 3 (a), (b), (c) and (d) show the XRD spectra of the pyrolyzed SPF resins at 1450°C and 1650°C under argon and nitrogen atmosphere respectively. In the case of PF resin, under different pyrolysis conditions (PF-1450-Ar, PF-1450-N_2, PF-1650-Ar and PF-1650-N_2), two broad diffraction peaks centred at 2θ = 24.9° and 43.2° were observed, which corresponds to (002) and (004) planes respectively of glassy carbon (PDF 89-8493). For PCTS modified PF samples pyrolyzed at 1450°C and 1650°C under argon atmosphere [Figure 3 (a) and (c)], in addition to the peaks at 2θ = 24.9° and 43.2°, well defined crystalline peaks attributable to β-SiC at 2θ = 35.6° (111), 41.3° (200), 59.9° (220), 71.7° (311) (PDF 74- 2307) and a small peak at 2θ = 33.7° corresponding to stacking faults in β-SiC were also observed [29]. Moreover, the intensity of the β-SiC peak increased with an increase in the concentration of PCTS. Interestingly, under a nitrogen atmosphere at 1450°C [Figure 3 (b)] these additional peaks [2θ = 35.6° (111), 41.3° (200), 59.9° (220), 71.7° (311), 75.4° (222)] were not observed and ceramic phase remained amorphous. The reason for the amorphous nature in the case of nitrogen atmosphere at 1450°C has been explained with the support FESEM analysis *(Section 3.2.3)*. With increase in the pyrolysis temperature from 1450°C to 1650°C, along with the additional peaks observed in the case of argon atmosphere, new peaks corresponding to β-Si_3N_4 were also observed at 2θ = 33.8° (002) and 38.3° (101) (PDF 33-1160) [Figure 3 (d)], which were not present in other systems. These Si_3N_4/SiC ceramic are reported to possess superior thermo-mechanical properties as compared to Si_3N_4 or SiC monolithic ceramic material [30, 31] and hence are highly desired ceramic for high-temperature applications. Also, these Si_3N_4/SiC ceramics are synthesized by controlling the pyrolysis conditions which is more efficient and facile than the conventional powder route. It was also observed that the peak at 2θ = 26.44° forms a shoulder peak with the main peak at 2θ = 24.9° corresponding to glassy carbon in all the

systems. This indicates the precipitation of graphitic carbon with increase in the concentration of PCTS. Moreover, this shoulder peak is sharper in the case of argon than nitrogen atmosphere which is supported by Raman analysis also.

3.2.2 Raman spectra of pyrolyzed SPF resin

The structural changes in the stoichiometrically excess carbon of pyrolyzed SPF resin with varying pyrolysis conditions were studied using Raman spectral analysis [Figure S3 (a), (b), (c) and (d)].

All the samples exhibited similar Raman spectra showing, disorder induced D and G' bands (overtone of D band) at ~1330 cm^{-1} and 2630 cm^{-1}, G band due to in-plane bond stretching of sp^2 carbon at ~1575 cm^{-1} and combinational D+D' band at ~2900 cm^{-1}. In addition to these peaks, some minor peaks corresponding to cubic 3C-SiC phases at 798 cm^{-1} and 930 cm^{-1} were also observed in some spectra [Figure S3 (a) and (c)]. Variations in position and intensity of D and G band, with changes in the structural organization of carbon phase in ceramics have been well reported [32-35]. Hence, by evaluating these parameters, the effect of pyrolysis conditions on the structural organization of carbon phase can be thoroughly investigated. These parameters were derived using Gaussian curve fitting of the Raman bands and are listed in Table 1 and Table 2. The relative intensity ratio of the D and G bands (I_D/I_G) are used to calculate excess carbon cluster size using the formula reported by Ferrari and Robertson [36]

$$\frac{I_D}{I_G} = C'(\lambda) L_a^2 \qquad (1)$$

where, L_a is the size of carbon domains along the six-fold ring plane and C' is a coefficient that depends on the excitation wavelength (λ) of the laser. The value of C' of the wavelength of 532 nm of the Nd: YAG laser used here is 0.6195 nm.

Table 1
Parameters derived from Raman spectra for ceramics derived from PF and SPF at 1450°C and 1650°C under argon atmosphere

Samples	Argon atmosphere							
	at 1450°C				at 1650°C			
	D peak position (cm^{-1})	G peak position (cm^{-1})	I_D/I_G	La (nm)	D peak position (cm^{-1})	G peak position (cm^{-1})	I_D/I_G	La (nm)
PF	1343	1571	1.32	1.45	1340	1572	1.35	1.47
SPF-5	1335	1572	1.30	1.44	1337	1564	1.29	1.44
SPF-10	1333	1572	1.27	1.43	1332	1571	1.28	1.43
SPF-15	1330	1573	1.23	1.40	1330	1571	1.36	1.48
SPF-20	1329	1574	1.19	1.38	1329	1574	1.44	1.52
SPF -25	1325	1575	1.33	1.46	1326	1577	1.53	1.57
SPF -30	1322	1575	1.56	1.58	1324	1584	1.59	1.60

Table 2
Parameters derived from Raman spectra for ceramics derived from PF and SPF at 1450°C and 1650°C under nitrogen atmosphere

Samples	Nitrogen atmosphere							
	at 1450°C				at 1650°C			
	D peak position (cm^{-1})	G peak position (cm^{-1})	I_D/I_G	La (nm)	D peak position (cm^{-1})	G peak position (cm^{-1})	I_D/I_G	La (nm)
PF	1346	1574	1.29	1.44	1339	1575	1.62	1.61
SPF-5	1330	1573	1.28	1.43	1333	1563	1.61	1.61
SPF-10	1348	1600	1.26	1.42	1332	1566	1.29	1.44
SPF-15	1346	1596	1.32	1.45	1326	1568	0.88	1.19
SPF-20	1337	1588	1.23	1.4	1325	1576	1.53	1.57
SPF -25	1346	1587	1.38	1.49	1322	1579	1.67	1.64
SPF -30	1330	1573	1.36	1.48	1322	1584	1.72	1.66

Increase in the frequency of G band or a decrease in the frequency of D band reflects the degree of orderness in carbon [34]. It was observed that, for SPF samples pyrolyzed at 1450°C and 1650°C under argon atmosphere, there was an increase in the G band frequency and decrease in the D band frequency with increase in PCTS concentration (Table 1). A similar trend in the D and G band frequency was also observed for SPF samples pyrolyzed at 1650°C under nitrogen atmosphere (Table 2). This indicates ordering of excess carbon from amorphous carbon to crystalline graphite with increase in PCTS concentration. On the contrary, for SPF samples pyrolyzed at 1450°C under nitrogen atmosphere (Table 2), no such trend in the D and G band frequency with PCTS concentration was observed, indicating insignificant effect of carbon phase at this pyrolysis temperature and gas atmosphere. More information on structural organization of carbon was obtained by calculating L_a.

For SPF samples pyrolyzed under argon atmosphere at 1450°C and 1650°C, initial decrease in L_a was observed followed by subsequent increase with increase in concentration of PCTS (Table 1). A similar trend in L_a values with PCTS concentration was also observed for SPF samples pyrolyzed at 1650°C under nitrogen atmosphere (Table 2). These results are in accordance with the Ferrari model [37], which explains that, for the transformation of amorphous carbon to crystalline graphite, rearrangement of distorted aromatic rings to six-membered ring occur, which results in the shrinkage of L_a, whereas, the in-plane growth of crystalline graphite will increase the L_a value. Contrastingly, for SPF samples pyrolyzed at 1450°C under nitrogen atmosphere, no trend in L_a values with PCTS concentration was observed (Table 2). This indicates that, at this pyrolysis temperature and gas atmosphere, excess carbon phase does not get affected significantly, which results in the formation of amorphous carbon, as supported by XRD results [Figure 3 (b)]. Thus, XRD and Raman results, revealed the existence of a strong

relationship between crystallization of ceramics and ordering of the excess carbon phase with employed pyrolysis conditions.

3.2.3 FESEM analysis of pyrolyzed SPF resin

XRD and Raman studies revealed that thermally more stable and desired ceramics are obtained under nitrogen atmosphere than argon atmosphere. In order to reveal the relationship between the thermal stability with employed pyrolysis conditions, morphological studies were carried out. The effect of pyrolysis conditions on the morphology of the ceramics was studied through FESEM analysis. It was observed that, the morphology of the obtained ceramics were highly sensitive to their processing pyrolysis atmospheres. The SPF samples pyrolyzed under argon atmosphere at both 1450°C and 1650°C displayed, two different morphologies viz. macro porous ceramics and nano-rod structured ceramics. These two different morphologies were obtained as a result of phase separation of ceramics under argon atmosphere. In-depth morphological investigations of these phase separated ceramics were done through FESEM and spot-EDAX analysis. Similar morphologies (Figure S5 and S6) were observed in all studied formulations (SPF-5, SPF-10, SPF-15, SPF-20, SPF-25 and SPF-30) and hence typical FESEM images are presented in Figure 4.

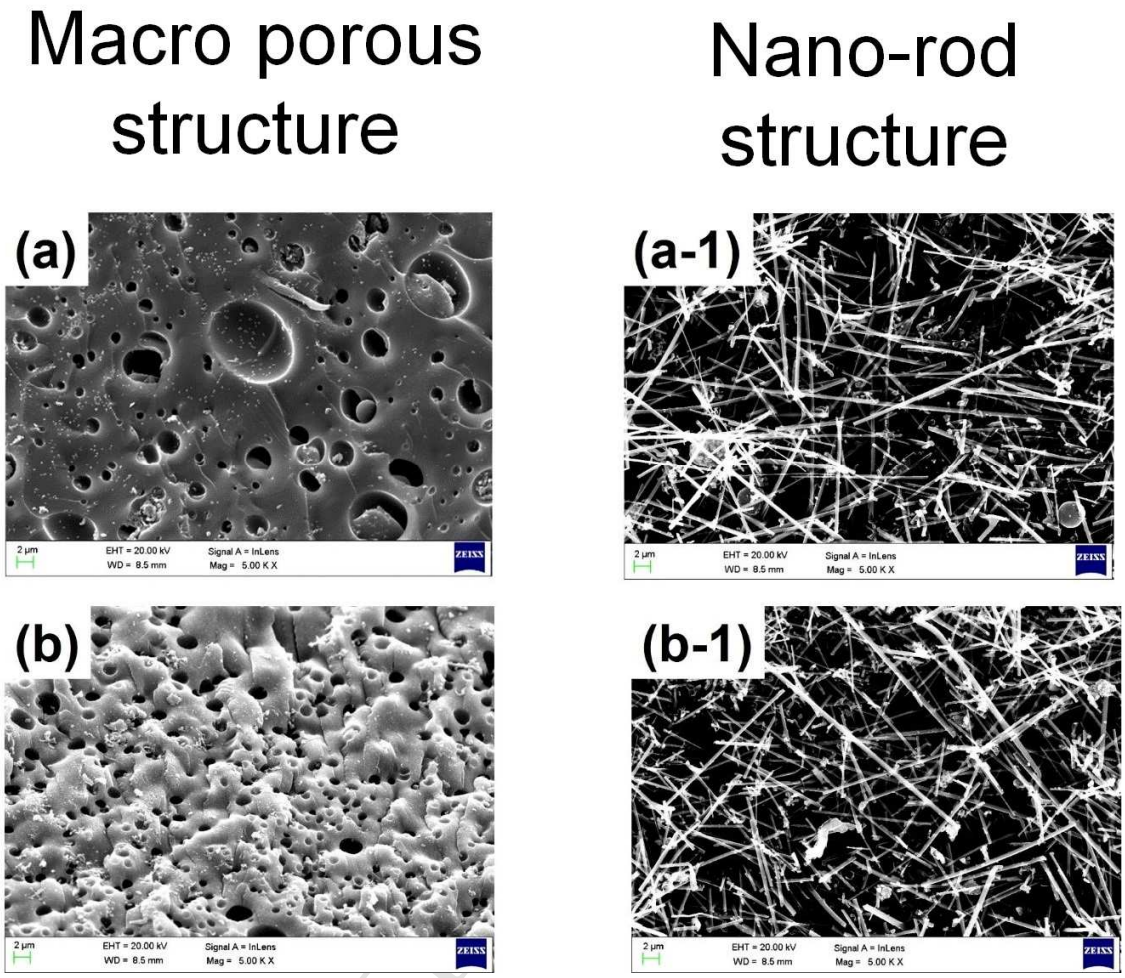

Figure 4. FESEM images of SPF pyrolyzed under argon atmosphere (a) at 1450°C and (b) at 1650°C

The formation of macro-porous ceramics can be explained by the decomposition of SiOCN ceramics [as shown in eqns. (2) to (6)] which results in local atomic rearrangement, forming a large number of Si-C enriched regions and gaseous species such as SiO, CO, N_2 and Si vapors, particularly at the range of 400°C to 650°C [38]. This is responsible for the formation of cracks and macro-pores structures through vapor-solid (VS) route mechanism.

$$SiC_xN_yO_{z(s)} \rightarrow SiC_{(s)} + N_{2(g)} + NO_{(g)} + CO_{(g)} + SiO_{(g)} + Si_{(g)} \quad (2)$$

$$Si_{(g)} + C_{(s)} \rightarrow SiC_{(s)} \quad (3)$$

$$2Si_{(g)} + 2CO_{(g)} \rightarrow 2SiC_{(s)} + O_{2(g)} \quad (4)$$

$$SiO_{(g)} + CO_{(g)} \rightarrow SiC_{(s)} + O_{2(g)} \quad (5)$$

$$SiO_{(g)} + C_{(s)} \rightarrow SiC_{(s)} + CO_{(g)} \quad (6)$$

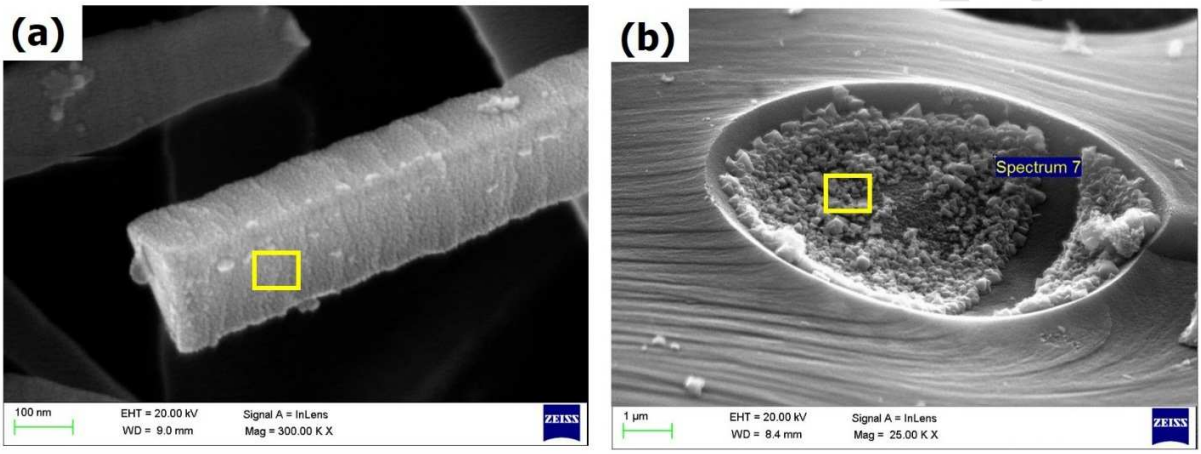

Figure 5 FESEM image at higher magnification of (a) SiC nano-rods under argon atmosphere and (b) nano-crystal decorated macro-porous cavity under nitrogen atmosphere

The chemical composition of nano-rod structured ceramics was determined using spot-EDAX analysis, which revealed that these nano-rods are composed of SiC ceramics with the elemental composition of $SiC_{4.6}O_{0.14}$. Further, FESEM image [Figure 5 (a)] shows these nano-rod structures are made of 1D triangular shaped with diameters ranging from 20 to 200 nm and lengths of about 4 µm. These nano-rod structured ceramics are formed by the reaction of oxygen with silicon and carbon [as shown in eqn. (4 & 5)]. This leads to the formation of SiO and CO gases which react with each other and get deposited in the form of nano-rods through vapor-vapor (VV) route mechanism [39-41]. Further, it is observed that, these nano-rods are made of 1D triangular shaped with diameters ranging from 20 to 200 nm and lengths of about 4 µm. As

per the literature [42], the growth of SiC nano-rods are preferentially grew along the [111] plane due to its thermodynamically feasible direction, hence 1D SiC nano-rod structures are formed during VV mechanism. These 1D nano-rod structured SiC ceramics are reported to have high potential in energy storage applications [43].

Conversely, under nitrogen atmosphere at both 1450°C and 1650°C, only macro porous ceramics were obtained with distinct variations in the morphology of the porous cavity. At 1450°C, empty macro-porous cavities were obtained (Figures S7) whereas at 1650°C nano-crystals decorated macro-porous cavities were obtained (Figures S8). Similar morphologies (Figure S7 and S8) were observed in all studied formulations (SPF-5, SPF-10, SPF-15, SPF-20, SPF-25 and SPF-30) and hence typical FESEM images are presented in Figure 6.

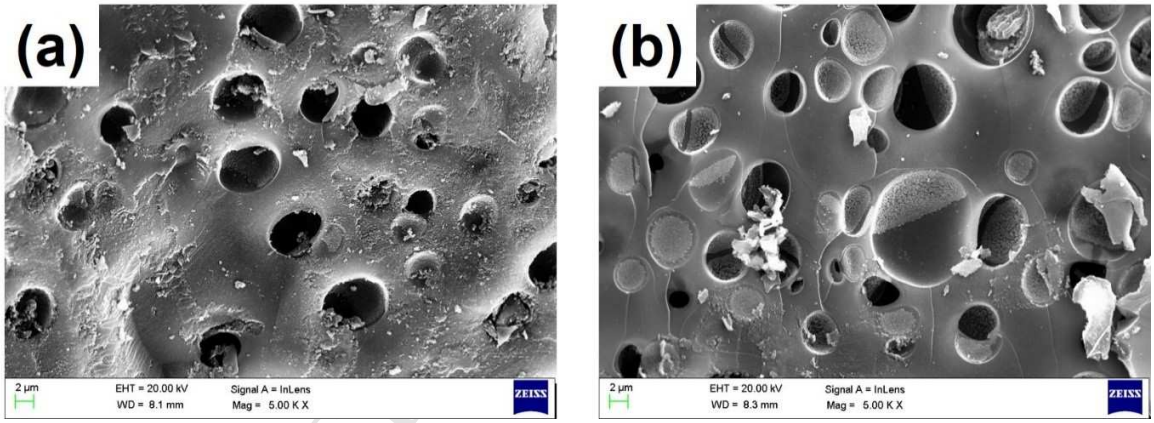

Figure 6. FESEM image of SPF pyrolyzed under nitrogen atmosphere (a) at 1450°C and (b) at 1650°C

The formation of the macro-porous ceramics at both 1450°C and 1650°C, can be explained again by the decomposition of SiOCN ceramics [as shown in eqns. (2) to (6)] which leads to the formation of macro-pores through VS route mechanism. Whereas, at 1650°C, the formation of nano-crystals decorated macro-porous cavity occurs through VV route mechanism which was understood by EDAX studies. Figure 5 (b) shows the FESEM micrograph of nano-

crystal decorated macro-porous cavity ceramics and the corresponding spot-EDAX analysis revealed that these nano-crystals are composed of SiC ceramics with the elemental composition of $SiC_{3.5}O_{0.09}$. These nano-crystals are formed by the chemical reaction between SiO and CO gases [as shown in eqn. (4 & 5)] which reacts with each other and gets deposited in the form of nano-crystals in macro-porous cavity through VV route mechanism as discussed previously. It is to be noted that, XRD spectra at 1650°C under nitrogen atmosphere showed the formation of Si_3N_4 ceramic along with SiC ceramics [Figure 3 (d)]. However, no nitrogen content was detected in the nano domain of the ceramics using spot-EDAX analysis. Hence, it can be concluded that the Si_3N_4 ceramics are embedded in the SiOCN matrix [42].

Interestingly it was observed that, under argon atmosphere, the reaction of SiO and CO gases leads to the formation of nano-rod structured ceramics, whereas under nitrogen atmosphere nano-crystals decorated macro-porous cavity ceramics were formed. In order to explain this difference in morphology, detailed investigations on variation in degree of porosity with PCTS concentration and employed pyrolysis conditions is mandatory. Figure 7 shows surface porosity values computed from FESEM image using ImageJ 1.46r software [26].

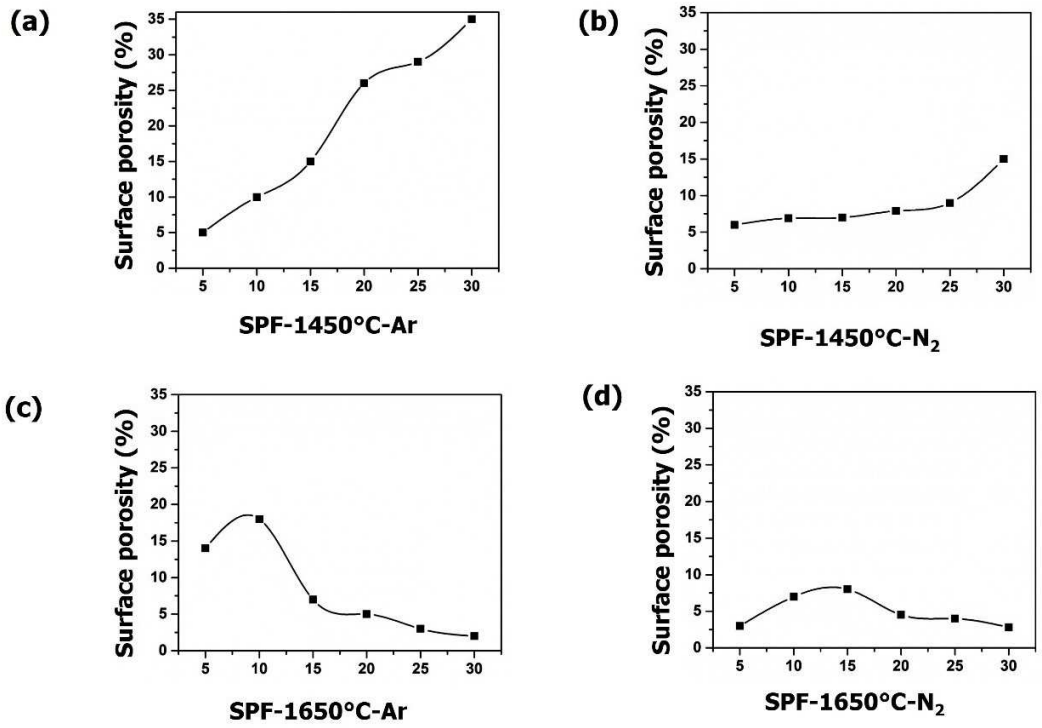

Figure 7. Variation of surface porosity with pyrolyzed SPF (a) at 1450°C under argon atmosphere, (b) at 1450°C under nitrogen atmosphere, (c) at 1650°C under argon atmosphere and (d) at 1650°C under nitrogen atmosphere

It was observed that, under argon atmosphere at both 1450°C and 1650°C [Figure 7 (a) & (c)], higher surface porosity was observed as compared to nitrogen atmosphere [Figure 7 (b) & (d)]. This clearly indicates that, the rate of decomposition of SiOCN ceramic is higher in argon atmosphere than nitrogen atmosphere. This difference in rate of decomposition of SiOCN ceramic is due to dual role of oxygen. As per previously reported literature [44], oxygen can inhibit as well as promote the decomposition of SiOCN ceramics. Along with nitrogen, oxygen inhibits the generation of -SiC_4- aggregates, delays the formation of β-SiC crystals, and hence maintains the amorphous state of SiOCN ceramics. On the contrary, in the reaction of oxygen with silicon and carbon, oxygen promotes the formation of SiO and CO gases accelerating the decomposition of SiOCN ceramics. These two factors mutually influence the stability of

amorphous SiOCN in different gas atmospheres. Under nitrogen atmosphere, the inhibition effects of oxygen and nitrogen on crystallization, play a major role in stabilization of SiOCN ceramic. While under argon atmosphere, the reaction of oxygen with silicon and carbon accelerates the vapor-phase reaction which leads to the crystallization of SiOCN ceramics.

As a result, degree of crystallinity of the glassy carbon was more in argon atmosphere as compared to nitrogen atmosphere. Further, the rate of decomposition of SiOCN ceramic increases with increase in the concentration of PCTS, which increases the degree of orderness in carbon. This explains the reason for increase in the crystallinity of glassy carbon with increase in the concentration of PCTS and with employed pyrolysis conditions. This observation falls in line with XRD and Raman results, where degree of crystallinity was more in argon atmosphere as compared to nitrogen atmosphere.

Furthermore, under argon and nitrogen atmospheres at 1450°C, surface porosity increased with increasing PCTS concentration [Figure 7 (a) & (b)]. This is due to the higher rate of decomposition of SiOCN ceramics with increase in PCTS concentration which increases the surface porosity. However, at 1650°C, surface porosity initially increased and then gradually decreased with increasing PCTS concentration [Figure 9 (c) & (d)]. This can be explained through two different path ways depending on pyrolysis atmosphere as shown in Scheme 3.

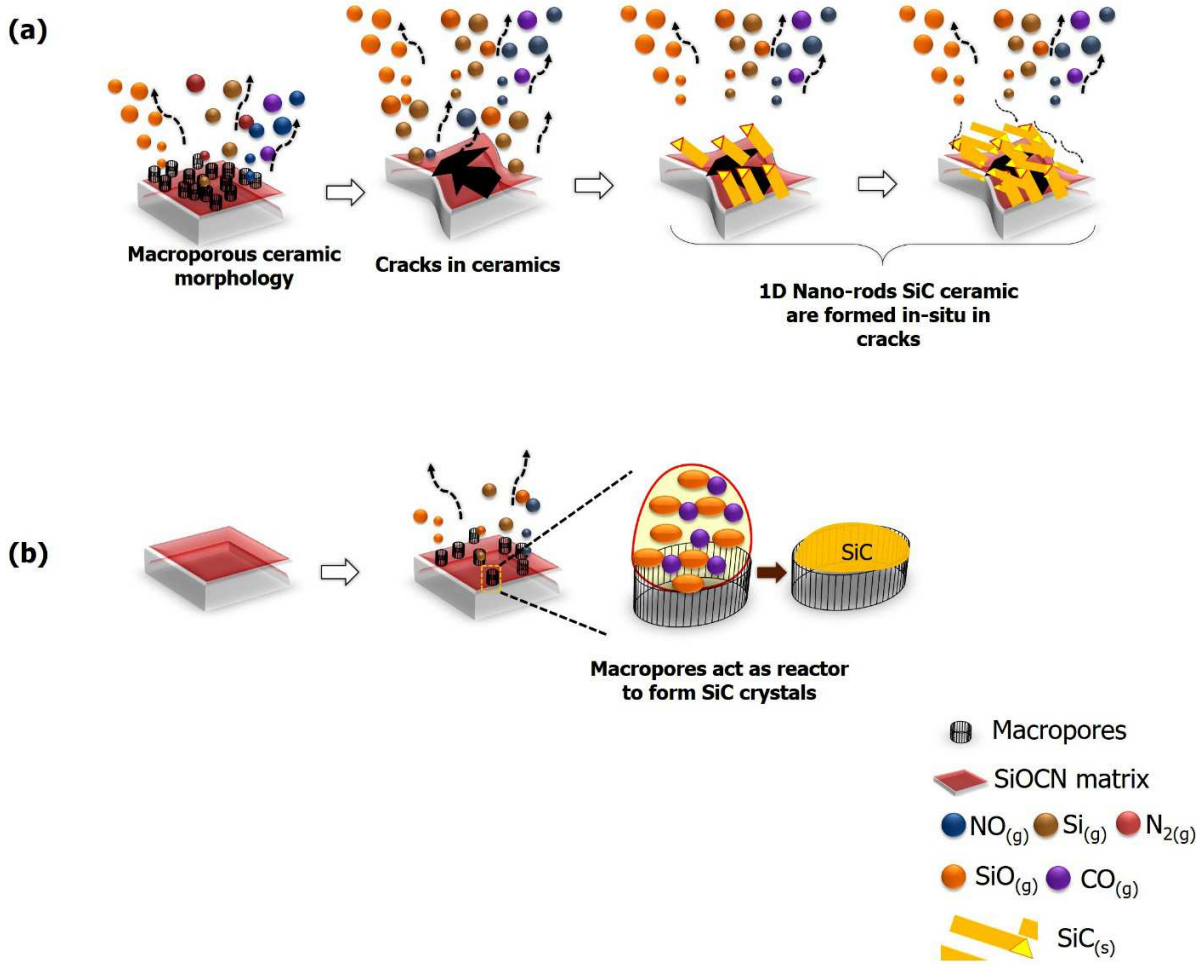

Scheme 3. Mechanism for the formation (a) nano-rod structured ceramic under argon atmosphere and (b) nano-crystal decorated macro-porous cavity ceramic under nitrogen atmosphere

Under argon atmosphere at 1650°C, rate of decomposition of SiOCN ceramic is higher which results in coalescence of macro pores and leads to the formation of cracks [Scheme 3 (a) & Figure S6 (f)]. These cracks form the path way for the VV mechanism which leads to *in-situ* formation of nano-rod structured SiC ceramics, which decreases the overall porosity of the ceramics. Conversely, under nitrogen atmosphere, the rate of decomposition is relatively slow and hence results in evolution of less number of gaseous molecules. In such a situation, the

macro-porous cavity acts as a reactor [Scheme 3 (b) & Figure S8 (f)] for the deposition of SiC nano-crystals which decreases the overall porosity of the ceramics. This also explains the reason for the formation of nano-rod structured ceramics under argon atmosphere, whereas nano-crystals decorated macro-porous cavity ceramics under nitrogen atmosphere.

3.2.4 Elemental analysis and Ceramic yield of pyrolyzed SPF resin

In order to further ascertain the elemental compositions of as obtained ceramics, wet chemical analysis method was employed [28]. Table 3 and 4 shows the elemental compositions of the pyrolyzed SPF resins at 1450°C and 1650°C under argon and nitrogen atmosphere.

Table 3
Elemental composition of ceramics derived from SPF at 1450°C and 1650°C under argon atmosphere

Samples	Argon atmosphere									
	at 1450°C					at 1650°C				
	Composition (wt. %)				Empirical formula normalized on Si	Composition (wt. %)				Empirical formula normalized on Si
	Si	C	N	O		Si	C	N	O	
PF	-	100	-	-	C	-	100	-	-	C
SPF-5	10	76	0.2	13	$Si_1C_{3.3}N_{0.01}O_{1.2}$	11	77	-	11	$Si_1C_{3.05}O_{0.9}$
SPF-10	14	73	0.2	12	$Si_1C_{2.2}N_{0.01}O_{0.7}$	15	75	-	10	$Si_1C_{2.14}O_{0.58}$
SPF-15	21	69	0.3	11	$Si_1C_{1.4}N_{0.01}O_{0.4}$	21	70	-	8	$Si_1C_{1.40}O_{0.34}$
SPF-20	25	66	0.3	8	$Si_1C_{1.1}N_{0.01}O_{0.3}$	27	67	-	6	$Si_1C_{1.06}O_{0.19}$
SPF -25	28	65	0.4	7	$Si_1C_1N_{0.01}O_{0.2}$	28	66	-	5	$Si_1C_{0.99}O_{0.14}$
SPF -30	33	62	0.5	5	$Si_1C_1N_{0.01}O_{0.1}$	32	65	-	2	$Si_1C_{0.85}O_{0.05}$

Table 4
Elemental composition of ceramics derived from SPF at 1450°C and 1650°C under nitrogen atmosphere

Samples	Nitrogen atmosphere									
	at 1450°C					at 1650°C				
	Composition (wt. %)				Empirical formula normalized on Si	Composition (wt. %)				Empirical formula normalized on Si
	Si	C	N	O		Si	C	N	O	
PF	-	100	-	-	C	-	100	-	-	C
SPF-5	7	71	1.4	19	$Si_1C_4N_{0.1}O_{2.1}$	8	72	1.3	17	$Si_1C_3N_{0.11}O_{1.7}$
SPF-10	10	70	2.2	18	$Si_1C_3N_{0.1}O_{1.5}$	12	70	1.3	15	$Si_1C_2N_{0.08}O_{1.1}$
SPF-15	15	65	2.8	16	$Si_1C_2N_{0.1}O_{1.0}$	16	67	1.4	14	$Si_1C_1N_{0.06}O_{0.7}$
SPF-20	18	63	3.1	15	$Si_1C_1N_{0.1}O_{0.7}$	20	64	2.0	14	$Si_1C_1N_{0.07}O_{0.6}$
SPF -25	22	62	3.6	11	$Si_1C_1N_{0.1}O_{0.4}$	21	65	2.3	11	$Si_1C_1N_{0.08}O_{0.4}$
SPF -30	26	59	4.7	10	$Si_1C_1N_{0.1}O_{0.3}$	28	60	2.5	9	$Si_1C_1N_{0.06}O_{0.3}$

At both the pyrolysis conditions (at 1450°C and 1650°C under argon and nitrogen atmosphere), it was found that the silicon and nitrogen content increases whereas that of oxygen and carbon decreases with increase in PCTS concentration. However, there were distinct differences in nitrogen content under argon and nitrogen atmosphere. Under argon atmosphere at 1450°C only trace amount of nitrogen content was observed. With increase in pyrolysis temperature to 1650°C no nitrogen content was found (Table 3). Conversely, under nitrogen atmosphere at both 1450°C and 1650 °C, higher nitrogen content was obtained (Table 4). These differences in nitrogen content with respect to pyrolysis gas atmosphere is due to higher rate of decomposition of SiOCN ceramics under argon atmosphere than nitrogen atmosphere. These observation reveals the reason for the formation of only SiC ceramics under argon atmosphere and desired Si_3N_4/SiC ceramics under nitrogen atmosphere. The ceramic yield of these obtained ceramics is another important criterion for high-temperature applications. Table 5 shows the variations in ceramic yield with pyrolysis condition and PCTS concentration.

Table 5
Ceramic yield of pyrolyzed SPF at 1450°C and 1650°C under argon and nitrogen atmosphere

Samples	Ceramic yield (wt. %)			
	Argon		Nitrogen	
	at 1450°C	at 1650°C	at 1450°C	at 1650°C
PF	35	32	36	33
SPF-5	37	35	43	41
SPF-10	38	36	45	43
SPF-15	39	36	49	46
SPF-20	39	37	54	52
SPF-25	42	38	57	54
SPF-30	42	40	63	60

It was observed that, at both the pyrolysis conditions (at 1450°C and 1650°C under argon and nitrogen atmosphere) ceramic yield increases with increase in PCTS concentration. Under argon atmosphere, highest ceramic residue of 42 wt. % and 41 wt. % for SPF-30 was obtained at 1450°C and 1650°C, respectively. While, under nitrogen atmosphere highest ceramic residue of 63 wt. % and 60 wt. % for SPF-30 was obtained at 1450°C and 1650°C, respectively. This shows that higher ceramic yield was achieved under nitrogen atmosphere as compared to argon atmosphere. This difference in ceramic yield is due to higher rate of decomposition of SiOCN ceramics under argon atmosphere than nitrogen atmosphere. Thus, the study reveals that under nitrogen atmosphere desired C/Si_3N_4/SiC ceramics are formed with higher ceramic yield (60 wt. %), whereas under argon atmosphere only C/SiC ceramics are formed with lower ceramic yield (40 wt. %). Hence, nitrogen atmosphere is a more suitable pyrolysis gas atmosphere than argon atmosphere.

4. Conclusions

The present study reports the synthesis and pyrolysis of new class of preceramic polymer based on SPF. The thermal transformation of SPF resin to ceramics were carried out under different pyrolysis conditions (at 1450°C and 1650°C under argon and nitrogen atmosphere).

Under argon atmosphere at both 1450°C and 1650°C, crystalline ceramics were obtained with only SiC as ceramic phase. Also, with increase in the concentration of PCTS, increase in degree of graphitization was observed, indicating significant structural rearrangement of excess carbon.

Under nitrogen atmosphere at 1450°C, amorphous ceramics were obtained with no structural re-organization of carbon. While, at 1650°C crystalline SiC and Si_3N_4 ceramic phases were obtained. Also, graphitization of excess carbon from amorphous carbon to crystalline graphite occurs, showing structural re-organization of excess carbon. Moreover, under nitrogen atmosphere at both 1450°C and 1650°C, only macro-porous ceramics were formed. In contrast to nitrogen atmosphere, in argon atmosphere at both 1450°C and 1650°C, additional 1D, triangular shaped, nano-rod structured ceramics along with macro-porous structure were formed. EDAX analysis revealed that these nano-rods are composed of SiC formed through VV route mechanism.

This study demonstrates SPF as a new class of preceramic polymer for high-temperature applications. The study also reveals that nitrogen atmosphere is a more suitable pyrolysis gas atmosphere than argon atmosphere for preparation of desired C/Si_3N_4/SiC ceramics with higher ceramic yield. Moreover, the work also represents an interesting and efficient route for synthesis of C/Si_3N_4/SiC ceramics by controlling the pyrolysis conditions which is way more facile than the conventional powder route.

Acknowledgement

The authors thank the authorities of VSSC for granting permission to publish this work. One of the authors (Ganesh Babu T.) is thankful to Indian Space Research Organization (ISRO) for the research fellowship. Help received from the members of the Analytical and Spectroscopy Division (ASD) for the thermal, chemical and spectral analyses is gratefully acknowledged.

References

[1] S. Schmidt, S. Beyer, H. Knabe, H. Immich, R. Meistring, A. Gessler, Advanced ceramic matrix composite materials for current and future propulsion technology applications, Acta Astronautica, 55 (2004) 409-420.

[2] N.P. Bansal, Handbook of ceramic composites, Springer Science & Business Media, 2006.

[3] F. Christin, Design, fabrication, and application of thermostructural composites (TSC) like C/C, C/SiC, and SiC/SiC composites, Advanced engineering materials, 4 (2002) 903-912.

[4] G. Mera, A. Navrotsky, S. Sen, H.-J. Kleebe, R. Riedel, Polymer-derived SiCN and SiOC ceramics–structure and energetics at the nanoscale, Journal of Materials Chemistry A, 1 (2013) 3826-3836.

[5] M. Graczyk-Zajac, G. Mera, J. Kaspar, R. Riedel, Electrochemical studies of carbon-rich polymer-derived SiCN ceramics as anode materials for lithium-ion batteries, Journal of the European Ceramic Society, 30 (2010) 3235-3243.

[6] Y. Gao, G. Mera, H. Nguyen, K. Morita, H.-J. Kleebe, R. Riedel, Processing route dramatically influencing the nanostructure of carbon-rich SiCN and SiBCN polymer-derived ceramics. Part I: Low temperature thermal transformation, Journal of the European Ceramic Society, 32 (2012) 1857-1866.

[7] G. Ziegler, H.-J. Kleebe, G. Motz, H. Müller, S. Traßl, W. Weibelzahl, Synthesis, microstructure and properties of SiCN ceramics prepared from tailored polymers, Materials chemistry and physics, 61 (1999) 55-63.

[8] N. Liao, W. Xue, H. Zhou, M. Zhang, Atomistic investigation of structural and mechanical properties of silicon carbon nitride with different SiC/Si3N4 ratios, Materials Chemistry and Physics, 143 (2013) 223-227.

[9] G. Mera, R. Riedel, F. Poli, K. Müller, Carbon-rich SiCN ceramics derived from phenyl-containing poly (silylcarbodiimides), Journal of the European Ceramic Society, 29 (2009) 2873-2883.

[10] W. Toreki, C.D. Batich, M.D. Sacks, A.A. Morrone, Synthesis and applications of a vinylsilazane preceramic polymer, 14th Annual Conference on Composites and Advanced Ceramic Materials, Part 2 of 2: Ceramic Engineering and Science Proceedings, Volume 11, Issue 9/10, Wiley Online Library, 1990, pp. 1371-1386.

[11] T. Ganesh Babu, R. Devasia, Boron-modified phenol formaldehyde resin-based self-healing matrix for Cf/SiBOC composites, Advances in Applied Ceramics, (2016) 1-13.

[12] H.K. Nason, Silicon modified phenolic resins and process for producing same, Google Patents, 1939.

[13] Y. Zhang, S. Shen, Y. Liu, The effect of titanium incorporation on the thermal stability of phenol-formaldehyde resin and its carbonization microstructure, Polymer degradation and stability, 98 (2013) 514-518.

[14] G.H. Hsiue, S.J. Shiao, H.F. Wei, W.J. Kuo, Y.A. Sha, Novel phosphorus-containing dicyclopentadiene-modified phenolic resins for flame-retardancy applications, Journal of applied polymer science, 79 (2001) 342-349.

[15] U. Hong, S. Jung, K. Cho, M. Cho, S. Kim, H. Jang, Wear mechanism of multiphase friction materials with different phenolic resin matrices, Wear, 266 (2009) 739-744.

[16] C.R. Nair, Advances in addition-cure phenolic resins, Progress in Polymer Science, 29 (2004) 401-498.

[17] J.-M. Lin, C.-C.M. Ma, Thermal degradation of phenolic resin/silica hybrid ceramers, Polymer degradation and stability, 69 (2000) 229-235.

[18] S.-C. Xu, N.-L. Zhang, J.-F. Yang, B. Wang, C.-Y. Kim, Silicon carbide-based foams derived from foamed SiC-filled phenolic resin by reactive infiltration of silicon, Ceramics International, 42 (2016) 14760-14764.

[19] C. Li, Z. Ma, X. Zhang, H. Fan, J. Wan, Silicone-modified phenolic resin: Relationships between molecular structure and curing behavior, Thermochimica Acta, 639 (2016) 53-65.

[20] A. Najafi, F. Golestani-Fard, H. Rezaie, Improvement of SiC nanopowder synthesis by sol–gel method via TEOS/resin phenolic precursors, Journal of Sol-Gel Science and Technology, 75 (2015) 255-263.

[21] A. Noparvar-Qarebagh, H. Roghani-Mamaqani, M. Salami-Kalajahi, Novolac phenolic resin and graphene aerogel organic-inorganic nanohybrids: High carbon yields by resin modification and its incorporation into aerogel network, Polymer degradation and stability, 124 (2016) 1-14.

[22] S. Li, F. Chen, B. Zhang, Z. Luo, H. Li, T. Zhao, Structure and improved thermal stability of phenolic resin containing silicon and boron elements, Polymer degradation and stability, (2016).

[23] D. Bahloul, M. Pereira, P. Goursat, N. Yive, R.J. Corriu, Preparation of Silicon Carbonitrides from an Organosilicon Polymer: I, Thermal Decomposition of the Cross-linked Polysilazane, Journal of the American Ceramic Society, 76 (1993) 1156-1162.

[24] D. Bahloul, M. Pereira, P. Goursat, Preparation of silicon carbonitrides from an organosilicon polymer: II, thermal behavior at high temperatures under argon, Journal of the American Ceramic Society, 76 (1993) 1163-1168.

[25] K.K. Chawla, Ceramic matrix composites, Composite Materials, Springer, 1998, pp. 212-251.

[26] D. Sreekanth, N. Rameshbabu, K. Venkateswarlu, Effect of various additives on morphology and corrosion behavior of ceramic coatings developed on AZ31 magnesium alloy by plasma electrolytic oxidation, Ceramics International, 38 (2012) 4607-4615.

[27] C.A. Schneider, W.S. Rasband, K.W. Eliceiri, NIH Image to ImageJ: 25 years of image analysis, Nat methods, 9 (2012) 671-675.

[28] F. D. Snell and C. L. Hilton, Encyclopedia of industrial chemical analysis., Journal of Pharmaceutical Sciences, 55 (1966) 993-994.

[29] D. Gosset, C. Colin, A. Jankowiak, T. Vandenberghe, N. Lochet, X-ray Diffraction Study of the Effect of High-Temperature Heat Treatment on the Microstructural Stability of Third-Generation SiC Fibers, Journal of the American Ceramic Society, 96 (2013) 1622-1628.

[30] H. Schmidt, G. Borchardt, A. Müller, J. Bill, Formation kinetics of crystalline Si3N4/SiC composites from amorphous Si–C–N ceramics, Journal of Non-Crystalline Solids, 341 (2004) 133-140.

[31] M. Hnatko, D. Galusek, P. Šajgalík, Low-cost preparation of Si 3 N 4–SiC micro/nano composites by in-situ carbothermal reduction of silica in silicon nitride matrix, Journal of the European Ceramic Society, 24 (2004) 189-195.

[32] S. Trassl, G. Motz, E. Rössler, G. Ziegler, Characterization of the Free-Carbon Phase in Precursor-Derived Si-C-N Ceramics: I, Spectroscopic Methods, Journal of the American Ceramic Society, 85 (2002) 239-244.

[33] G. Mera, A. Tamayo, H. Nguyen, S. Sen, R. Riedel, Nanodomain Structure of Carbon-Rich Silicon Carbonitride Polymer-Derived Ceramics, Journal of the American Ceramic Society, 93 (2010) 1169-1175.

[34] S. Trassl, H.J. Kleebe, H. Störmer, G. Motz, E. Rössler, G. Ziegler, Characterization of the Free-Carbon Phase in Si-C-N Ceramics: Part II, Comparison of Different Polysilazane Precursors, Journal of the American Ceramic Society, 85 (2002) 1268-1274.

[35] S. Trabl, D. Suttor, G. Motz, E. Rössler, G. Ziegler, Structural characterisation of silicon carbonitride ceramics derived from polymeric precursors, Journal of the European Ceramic Society, 20 (2000) 215-225.

[36] A.C. Ferrari, J. Robertson, Raman spectroscopy of amorphous, nanostructured, diamond–like carbon, and nanodiamond, Philosophical Transactions of the Royal Society of London A: Mathematical, Physical and Engineering Sciences, 362 (2004) 2477-2512.

[37] A.C. Ferrari, J. Robertson, Interpretation of Raman spectra of disordered and amorphous carbon, Physical review B, 61 (2000) 14095.

[38] C. Vakifahmetoglu, I. Menapace, A. Hirsch, L. Biasetto, R. Hauser, R. Riedel, P. Colombo, Highly porous macro-and micro-cellular ceramics from a polysilazane precursor, Ceramics International, 35 (2009) 3281-3290.

[39] Y. Gao, Y. Bando, K. Kurashima, T. Sato, The microstructural analysis of SiC nanorods synthesized through carbothermal reduction, Scripta materialia, 44 (2001) 1941-1944.

[40] Y. Gao, Y. Bando, K. Kurashima, T. Sato, SiC nanorods prepared from SiO and activated carbon, Journal of materials science, 37 (2002) 2023-2029.

[41] T. Hata, S. Bonnamy, P. Bronsveld, V. Castro, M. Fujisawa, H. Kikuchi, Y. Imamura, SiC Nanorods grown on SiC coated Wood Charcoal.

[42] C. Vakifahmetoglu, Fabrication and properties of ceramic 1D nanostructures from preceramic polymers: a review, Advances in Applied Ceramics, 110 (2011) 188-204.

[43] I.K. Sung, Christian, M. Mitchell, D.P. Kim, P.J.A. Kenis, Tailored Macroporous SiCN and SiC Structures for High-Temperature Fuel Reforming, Advanced Functional Materials, 15 (2005) 1336-1342.

[44] M. Monthioux, O. Delverdier, Thermal behavior of (organosilicon) polymer-derived ceramics. V: Main facts and trends, Journal of the European Ceramic Society, 16 (1996) 721-737.

Highlights

- The study reports synthesis and pyrolysis of novel preceramic polymer based on SPF
- The thermal transformation was carried out under different pyrolysis conditions
- N_2 atmosphere gives desired C/SiC/Si_3N_4 ceramics with high ceramic yield